From Monodisperse Sulfurized Palladium Nanoparticles to Tiara Pd(II) Thiolate Clusters: Influence of Thiol Ligand on Thermal Treatment of a Palladium(II)−Amine System

Zhiqiang Yang, Kenneth J. Klabunde,* and Christopher M. Sorensen

Departments of Chemistry and Physics, Kansas State University, Manhattan, Kansas 66506

Received: August 15, 2007; In Final Form: September 21, 2007

In the present research, the influence of dodecanethiol on product distribution upon heating a Pd(II)−octylamine system was investigated. The molar ratio of octylamine to Pd(II) was fixed at 20:1, and the concentration of dodecanethiol was changed systematically, which resulted in different final products. Without the thiol ligand, only aggregated Pd(0) particles were obtained due to the reduction of Pd(II) by octylamine. When the molar ratio of dodecanethiol to Pd(II) was increased to 0.5, highly monodisperse sulfurized palladium nanoparticles with a diameter of 7.55 ± 0.73 nm were generated. Continually increasing the molar ratio led to mixed products composed of decreasing amounts of sulfurized palladium nanoparticles plus increasing amounts of a Pd(II)−thiolate complex. When the molar ratio reached 2, only the thiolate complex was found as the final product, which was further characterized and then proven to be a tiara Pd(II) thiolate cluster compound, $[Pd(SC_{12}H_{25})_2]_6$, that has been described in one of our earlier papers.[1]

Introduction

Organic ligands with long C chains such as alkyl carboxyl acids, alkylthiols, alkylamines, and phosphines are widely applied as protecting agents to synthesize monolayer-protected clusters (MPC) of metal, metal oxide, metal chalcogenide, etc. According to the literature, the functions of these ligands may be more complicated than the obvious chemical adsorption on the particle surface. The digestive ripening method established in our lab indicates that pre-prepared polydisperse metal particles can react with certain organic ligands and then transform to highly monodisperse nanoparticles.[2−4] For systems where the ligands are added before the formation of nanoparticles, it is possible that metal ion−ligand complexes (coordination compounds) form initially, followed by chemical reactions that lead to nanoparticles. In some cases, the ligands may undergo decomposition and release certain components to form the nanoparticles. For example, metal sulfides such as NiS and Cu_2S with controllable shapes (nanorod, nanosphere, or nanoprism) have been synthesized through thermolysis of the corresponding metal thiolates;[5,6] a variety of metal oxide nanoparticles has been produced by the decomposition of metal oleate complexes;[7,8] and nanorods of metal phosphides including MnP, Co_2P, FeP, and Ni_2P have been prepared via the thermal decomposition of metal−phosphine complexes.[9] In these cases, the ligands serve as both the protecting agents and the source materials for S, O, and P. Furthermore, to achieve the best control over particle size, shape, and size distribution, mixed ligands are generally employed, which makes the situation more complicated. In most cases, the functions of each ligand in a ligand−mixed system are not completely specified.

As highly active catalysts with an enlarged surface area, Pd nanoparticles have been attracting attention, and some preparation methods have been established. Reducing agents such as lithium triethylborohydride (Superhydride),[10] lithium borohydride,[11] sodium borohydride,[12] hydrazine,[13] and sodium hypophosphite[14] are generally applied to convert Pd(II) ions to Pd metal. The reduction can also be achieved by refluxing Pd(II) in an ethanol/water solution.[15−17] To control the particle size and size distribution, a variety of protecting agents has been applied, including hydrophilic ones such as sodium dodecyl sulfate[14] and polyvinylpyrrolidone (PVP)[15,16] or hydrophobic ones such as alkanethiols[10,12,17] and phosphines.[18,19]

As mild reducing agents, alkylamines have been used to prepare gold and silver nanoparticles.[20] To the best of our knowledge, the amine-induced reduction of Pd(II) has not been reported. In this paper, the reduction of Pd(II) by octylamine and the influence of dodecanethiol on this process were investigated. The results provide a facile method to synthesize highly monodisperse sulfurized Pd nanoparticles, which are good catalysts for some reactions.[21,22] More importantly, it is a good example concerning how different ligands may play special roles in a ligand−mixed system and how either pure coordination compounds or monodisperse nanoparticles can be prepared based on this very simple approach.

Experimental Procedures

Materials. Sodium tetrachloropalladate(II) (99%), octylamine (99%), and 1-dodecanethiol (98%) were obtained from Aldrich. 4-*t*-Butyltoluene (96%) was purchased from Acros Organics. Other chemicals were purchased and used as received.

Thermolysis without Dodecanethiol. In a glass tube, 0.029 g of Na_2PdCl_4 (1.0×10^{-4} mol), 10 mL of 4-*t*-butyltoluene, and 0.33 mL of octylamine (2.0×10^{-3} mol) were added sequentially. The mixture was sonicated for 30 min to form a colorless solution. Then, the tube was connected to a vacuum line and an argon gas tank through a rubber septum equipped with needles. The mixture was degassed and then flushed with argon several times. After that, it was heated (about 192 °C) in a preheated sand bath for 1 h under the protection of argon. During that time, black precipitates were produced. After 1 h, the tube was removed from the sand bath and left to cool. Finally, the black precipitates were collected by centrifugation

* Corresponding author. Tel.: (785) 532-6849; fax: (785) 532-6666; e-mail: kenjk@ksu.edu.

10.1021/jp0765751 CCC: $37.00
Published on Web 11/16/2007

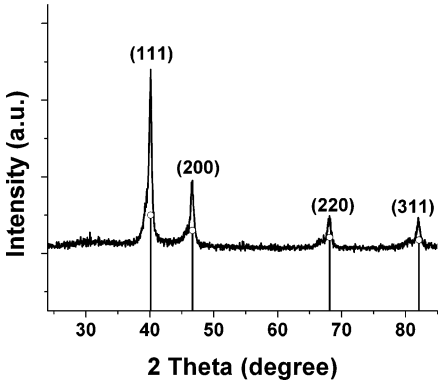

Figure 1. Powder XRD pattern of sample (0 X) indicating the formation of Pd(0) crystals. Standard pattern is based on JCPDS file 46-1043.

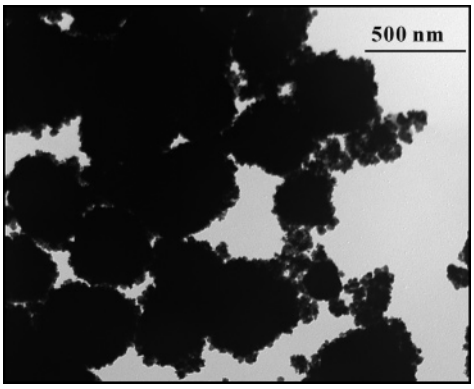

Figure 2. TEM image of sample (0 X) shows aggregated particles.

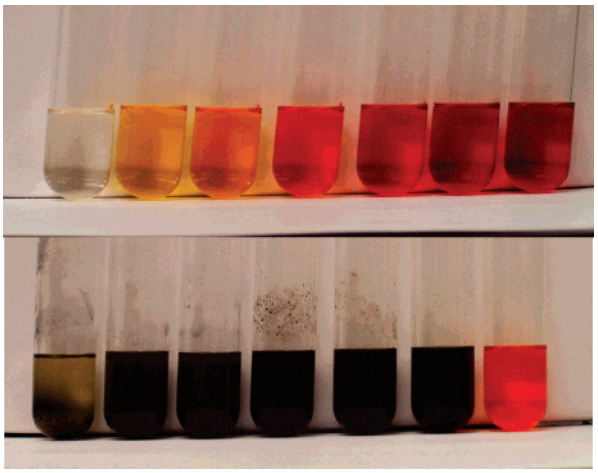

Figure 3. Solutions with different amounts of dodecanethiol before (upper) and after (lower) heating. Molar ratios of thiol to Pd(II) are 0, 0.125, 0.25, 0.5, 1, 1.5, and 2 from left to right.

and washed with 95% ethanol (30 mL × 4) and then pure ethanol (30 mL × 4).

Thermolysis with Different Amounts of Dodecanethiol. In a glass tube, 0.029 g of Na_2PdCl_4 (1.0×10^{-4} mol), 10 mL of 4-*t*-butyltoluene, 0.33 mL of octylamine (2.0×10^{-3} mol), and certain amounts of dodecanethiol were added sequentially. The molar ratios of thiol to Pd(II) were altered systematically from 0.125, 0.25, 0.5, 1, 1.5, to 2. After sonication for 30 min, the Pd(II) salt was dissolved, and the solution's color changed to yellow or orange−red, depending on the concentration of thiol. Then, the thermal reaction and product collection were carried out in the same way as described previously. For convenience,

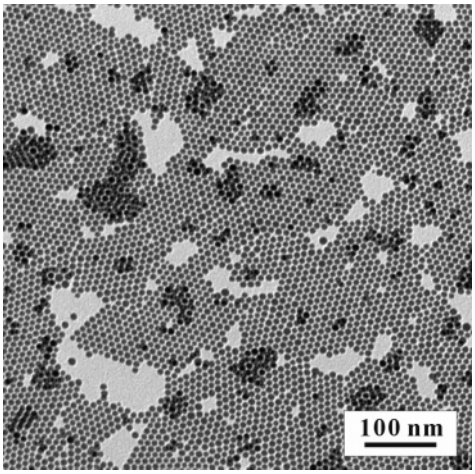

Figure 4. TEM image of sample (0.5 X).

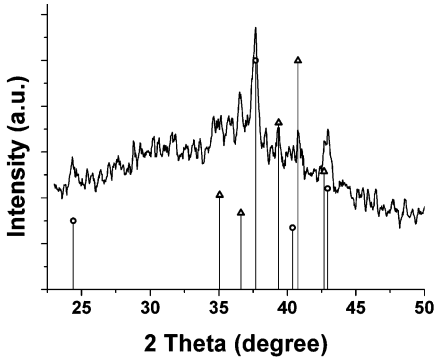

Figure 5. Powder XRD of sample (0.5 X). Standard patterns are from JCPDS files 30-884 ($Pd_{16}S_7$, marked with ○) and 73-1387 (Pd_4S, marked with Δ).

the obtained products are labeled as sample (*n* X) in this paper (*n* is the molar ratio of thiol to Pd(II) ion).

Equipment and Analysis. Transmission electron microscopy (TEM) was performed on a Philips CM100 microscope operated at 100 kV. To prepare a TEM sample, products were dispersed with toluene, and then a drop of solution was dropped onto a carbon-coated Formvar copper grid, which was allowed to dry in air. UV−vis absorption analysis was carried out on a Cary 500 UV−vis NIR spectrophotometer. IR spectra were obtained using a NEXUS 670 FT-IR system produced by the Nicolet Instrument Corporation. Powder X-ray diffraction (XRD) patterns were recorded by a Bruker D8 X-ray diffractometer with Cu Kα radiation. ^{1}H NMR spectra were obtained on a Varian Unity 400 Plus 400 MHz NMR system.

Results

Heating of Pd(II)−Octylamine Mixtures without Thiol. First, brown Na_2PdCl_4 powder and excess amounts of octylamine were added to 4-*t*-butyltoluene, which served as a high boiling point solvent. After sonication, the brown color of the Pd(II) salt faded, and a colorless solution formed. A likely explanation for this phenomenon is the formation of certain Pd(II)−amine complexes, which are colorless and soluble in the solvent. When heated at the boiling temperature of the solvent (192 °C), the system turned to black in minutes. After 1 h, black precipitates were obtained as sample (0 X). The powder XRD pattern of this sample indicates that pure fcc palladium crystals had been generated (Figure 1). The formation of Pd(0) is attributed to the reduction of Pd(II) by amine at high temperatures, in which the amine ligands are oxidized to nitriles.[23]

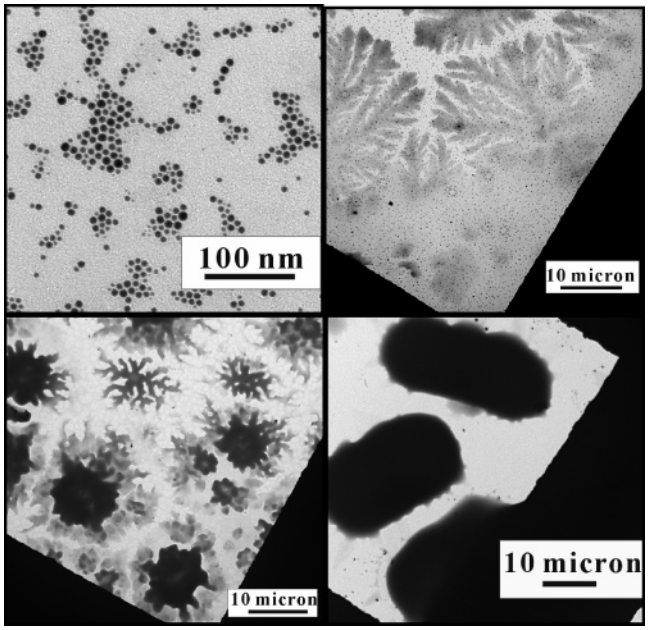

Figure 6. TEM images for sample (1 X) (upper row) and sample (1.5 X) and sample (2 X) (lower row, from left to right).

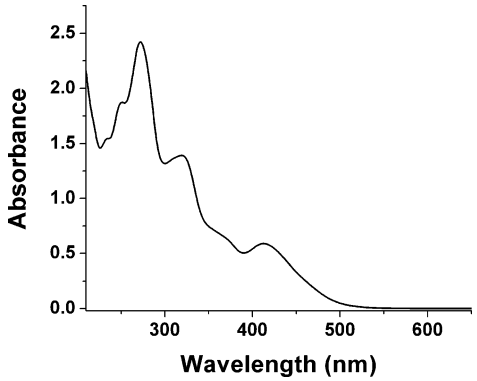

Figure 7. UV−vis pattern of sample (2 X) in *n*-heptane.

The reaction is assumed to occur according to the following equation:

$$2Na_2PdCl_4 + C_8H_{17}NH_2 \rightarrow Pd^0 + C_7H_{15}CN + 4NaCl + 4HCl$$

In support of this idea, a peak at 2239 cm^{-1} (the normal position for the CN stretching vibration) was found in the IR spectrum of the solution after heating.

A typical TEM image shows that the resulting crystallites aggregate into large roughly spherical particles at about 300−700 nm (Figure 2). This result is consistent with the observation of the reaction mixture after heating (i.e., the generated Pd(0) particles are not stable in the solution and ready to settle down as black precipitates).

Heating of Pd(II)−Octylamine−Dodecanethiol Systems. To investigate the influence of thiol ligands, different amounts of dodecanethiol were added (molar ratio of thiol/Pd(II): 0.125, 0.25, 0.5, 1, 1.5, and 2) before heating, while the molar ratio of octylamine/Pd(II) was fixed at 20. After sonication to dissolve the Pd(II) salt precursor, a series of solutions with the color changing from yellow to orange−red was obtained (Figure 3, upper row). As compared to the colorless solution of the Pd(II)−amine complex, it was obvious that certain colored Pd(II)−thiol complexes were generated.

After heating for 1 h, the solutions turned black for the systems with a molar ratio of thiol/Pd(II) ≤ 1.5, while the sample with a molar ratio equal to 2 remained as an orange−red solution (Figure 3, lower row). As seen in Figure 3, sample (0.125 X) and sample (0.25 X) were more stable than sample (0 X), but they still precipitated out of the solutions after days. TEM microphotos indicate the formation of smaller aggregated particles as compared to sample (0 X) (see Supporting Information Figure S1).

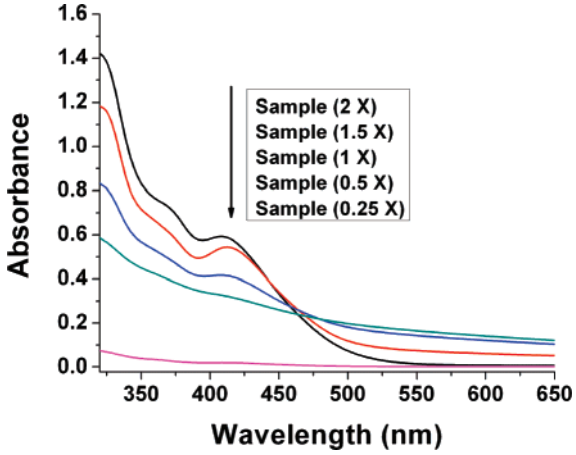

Figure 8. UV−vis patterns of solutions after heating (50 μL of solution in 3 mL of *n*-heptane).

When the molar ratio of thiol/Pd(II) was increased to 0.5, a stable black colloidal solution was obtained after heating, which could be stored in a capped vial for months without observable precipitates. TEM observation (Figure 4) demonstrates highly monodisperse nanoparticles, which self-assemble into a hexagonal close-packing pattern on the TEM grid like other monolayer-protected clusters. The average diameter of the particles was 7.55 ± 0.73 nm, with a standard deviation of 9.7% (see Supporting Information Figure S2 for the histogram pattern).

The powder XRD pattern (Figure 5) shows that the obtained nanoparticles are sulfurized palladium instead of pure Pd(0). Peaks standing for $Pd_{16}S_7$ and Pd_4S were found, and the former is dominating according to peak intensity. Elemental analysis (C: 18.28, H: 3.29, S: 11.65, Pd: 52.73, N: <0.5 in wt %) points out the high S content in the sample. If assuming that the nanoparticles are covered with $SC_{12}H_{25}$ species, a calculation based on the elemental analysis result indicates that the molar ratio of Pd/S in the particle cores is about 2.1. This value is close to that in $Pd_{16}S_7$ (2.3) and greatly consistent with the XRD results. Further calculation based on the particle size and density (estimated to be 7 g/cm^3) reveals that the composition of each nanoparticle is close to $(Pd_{16}S_7)_{14}(SC_{12}H_{25})_{57}$. Since there are no other S sources in the reaction system, the S in the particle cores is attributed to the decomposition of the thiol ligand. More details will be discussed later.

The solution color of sample (1 X) and sample (1.5 X) was not as dark as in sample (0.5 X). The optical density decreased with the increase of thiol ligand. Also, even though the basic color was black, an increase in the yellow−orange tint from sample (0.5 X) to sample (1.5 X) was noticeable. At the end, the solution of sample (2 X) was not dark at all and only exhibited an orange−red color. This trend can be seen more clearly when the samples were precipitated out of the solution with 95% ethanol. As compared to the black precipitates in sample (0.5 X), precipitates with brown, yellowish-brown, and bright orange color were obtained for sample (1 X), sample (1.5 X), and sample (2 X), respectively (see Supporting Information Figure S3). All of these observations strongly suggest that, with

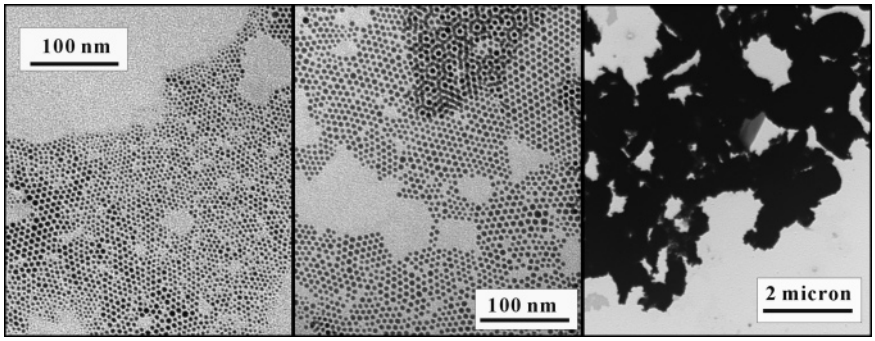

Figure 9. TEM images indicating growth of particles in sample (0.5 X) along with heating time (from left to right: 30 min, 45 min, and 2 h).

SCHEME 1: Different Products Controlled by Thiol Concentration[a]

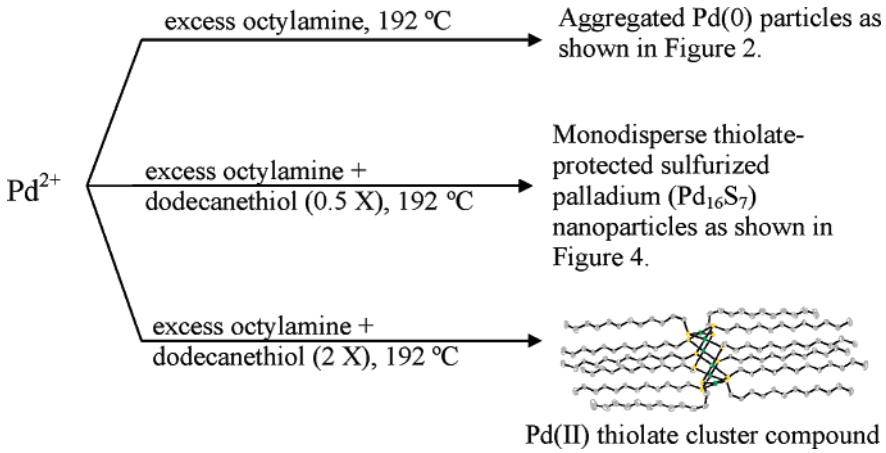

[a] Molecular structure of the cluster compound is from our early studies.[1]

an increase of dodecanethiol, the formation of nanoparticles will be hindered, and some orange species will become dominant in the final products.

The results from TEM confirm the viewpoint mentioned previously (Figure 6). The typical TEM image of sample (1 X) shows both nanoparticles with average diameters of about 6.5 nm and large snowflake-like patterns with a size in the dimension of tens of micrometers. For sample (1.5 X), smaller but much darker snowflake patterns and extremely small nanoparticles were observed. For sample (2 X), the TEM image indicates only rod-like patterns, and no nanoparticles can be found.

To understand the chemistry, sample (2 X) was collected as dry product and then characterized. The orange powder was not soluble in polar solvents such as ethanol or acetone but readily dissolved in nonpolar solvents such as hexanes or toluene. In the UV−vis spectrum of sample (2 X) (Figure 7), three main peaks are found at 272, 318, and 413 nm, which are consistent with the UV−vis features of a tiara Pd(II) thiolate complex, $[Pd(SC_{12}H_{25})_2]_6$, that has been fully characterized in our early studies.[1] This was further confirmed by comparing the ^{1}H NMR and powder XRD patterns of sample (2 X) (see Supporting Information Figures S4 and S5) with those data previously obtained from $[Pd(SC_{12}H_{25})_2]_6$. All the results have very good matches.

Discussion

Before heating, as good ligands, both octylamine and dodecanethiol could coordinate with Pd(II) ions to form soluble coordination complexes in the solvent. Without adding thiol, the solution of the Pd(II)−amine complex was colorless. When coordinated with dodecanethiol, it had a yellow to orange−red color depending on the thiol concentration. Since octylamine was in a large excess (20 X) and dodecanethiol was not enough in most cases ($\leq$2 X), the color change of the solutions also indicated that dodecanethiol was a much stronger ligand than octylamine. So, in any solution, Pd(II) ions strongly coordinate with dodecanethiol, but remaining coordination sites are filled by octylamine.

During heating, three main reactions could occur according to the experimental results. One was the amine-induced reduction of Pd(II) to Pd(0); the other was the formation of a tiara Pd(II) thiolate complex, $[Pd(SC_{12}H_{25})_2]_6$; and the third was the chemical adsorption and decomposition of Pd(II) thiolate species on the as-synthesized nanoparticles. In the case of sample (0 X), only the first reaction occurred, and aggregated Pd(0) particles were generated, which indicated that octylamine was not a good protecting ligand for the particles in this system. For sample (2 X), according to the experimental results, all of the Pd(II) ions were consumed to form $[Pd(SC_{12}H_{25})_2]_6$, and no reduction took place. This cluster compound has a stable sandwich-like ring structure and only undergoes decomposition at much higher temperatures.[1] For sample (0.125 X) to sample (1.5 X), since the amounts of dodecanethiol were limited, some Pd(II) ions were consumed to form $[Pd(SC_{12}H_{25})_2]_6$, while others were still reduced by octylamine. Along with the formation of Pd(0) particles, thiolate species were chemically adsorbed onto the particle surface. After adsorption, the thiolate species were not stable anymore, and the decomposition process occurred, which resulted in the sulfurization of Pd(0) nanoparticles. The control of the chemical paths by thiol concentration is indicated in Scheme 1. The breaking of the S−C bond in thiol ligands on as-synthesized palladium nanoparticles or films has also been reported by others.[24−26]

According to the sequence mentioned previously, the composition change in the final products is reasonable. Besides visual observations and TEM, the increase of $[Pd(SC_{12}H_{25})_2]_6$ in the final products with increasing dodecanethiol was further indicated by measuring the UV−vis absorbance of the solutions after heating, in which the featured peak at 413 nm of $[Pd(SC_{12}H_{25})_2]_6$ was employed (Figure 8).

It is obvious that sample (2 X) has the highest concentration of $[Pd(SC_{12}H_{25})_2]_6$, followed by sample (1.5 X) and sample (1 X) due to the partial adsorption and decomposition. In sample (0.5 X), this peak disappears, and the pattern only reflects the scattering effects of the nanoparticles. This means that almost all of $[Pd(SC_{12}H_{25})_2]_6$ has been consumed. The overall results are the formation of thiolate-protected sulfurized palladium nanoparticles as shown in Figure 4. If this sample is heated for another 1 h, aggregation of the nanoparticles will happen due to the further decomposition of the adsorbed thiolates. The evolution of the particles along with heating time in sample (0.5 X) is shown in Figure 9 (also see Figure 4 for the TEM image of the sample at 1 h). For sample (0.25 X), the UV−vis pattern indicates that no $[Pd(SC_{12}H_{25})_2]_6$ exists and that the scattering effects are also low due to the large size of the obtained particles.

A similar influence of thiol ligands on the synthesis of Pd(0) nanoparticles using $NaBH_4$ as a reducing agent was reported previously.[12] With an increasing thiol concentration, the final products changed from thiolate-protected nanoparticles to certain Pd(II) thiolate complexes. For other metal ions, Lin et al. reported the influence of oleic acid on the growth of Co(0) nanocrystals.[27] Increasing the concentration of oleic acid also resulted in the transformation action from Co(0) nanoparticles to Co(II) cluster compounds. The results described herein add to our understanding of these sensitive chemical processes that are ligand controlled.

Conclusion

In this paper, we report the influence of a thiol ligand on the formation of Pd nanoparticles through amine-induced reduction. When increasing the concentration of thiol, the final products changed from monodisperse sulfurized palladium nanoparticles (7.55 ± 0.73 nm), to a mixture of nanoparticles and Pd(II) thiolate complex, $[Pd(SC_{12}H_{25})_2]_6$, and then to the pure complex at last.

Acknowledgment. We thank the biology department of Kansas State University for use of the TEM facilities. Thanks are also given to Dr. Alexander B. Smetana for the helpful discussion.

Supporting Information Available: TEM images of sample (0.125 X) and sample (0.25 X); histogram of sample (0.5 X); photo indicating different color when precipitated with 95% ethanol for sample (0.5 X) to sample (2 X); and ^{1}H NMR and powder XRD patterns for sample (2 X). This material is available free of charge via the Internet at http://pubs.acs.org.

References and Notes

(1) Yang, Z.; Smetana, A. B.; Sorensen, C. M.; Klabunde, K. J. *Inorg. Chem.* **2007**, *46*, 2427−2431.
(2) Prasad, B. L. V.; Stoeva, S. I.; Sorensen, C. M.; Klabunde, K. J. *Chem. Mater.* **2003**, *15*, 935−942.
(3) Smetana, A. B.; Klabunde, K. J.; Sorensen, C. M. *J. Colloid Interface Sci.* **2005**, *284*, 521−526.
(4) Stoeva, S.; Klabunde, K. J.; Sorensen, C. M.; Dragieva, I. *J. Am. Chem. Soc.* **2002**, *124*, 2305−2311.
(5) Ghezelbash, A.; Sigman, M. B., Jr.; Korgel, B. A. *Nano Lett.* **2004**, *4*, 537−542.
(6) Larsen, T. H.; Sigman, M.; Ghezelbash, A.; Doty, R. C.; Korgel, B. A. *J. Am. Chem. Soc.* **2003**, *125*, 5638−5639.
(7) Jana, N. R.; Chen, Y.; Peng, X. *Chem. Mater.* **2004**, *16*, 3931−3935.
(8) Jun, Y.-w.; Choi, J.-s.; Cheon, J. *Angew. Chem., Int. Ed.* **2006**, *45*, 3414−3439.
(9) Park, J.; Koo, B.; Yoon, K. Y.; Hwang, Y.; Kang, M.; Park, J.-G.; Hyeon, T. *J. Am. Chem. Soc.* **2005**, *127*, 8433−8440.
(10) Yee, C. K.; Jordan, R.; Ulman, A.; White, H.; King, A.; Rafailovich, M.; Sokolov, J. *Langmuir* **1999**, *15*, 3486−3491.
(11) Martin, J. E.; Wilcoxon, J. P.; Odinek, J.; Provencio, P. *J. Phys. Chem. B* **2002**, *106*, 971−978.
(12) Zamborini, F. P.; Gross, S. M.; Murray, R. W. *Langmuir* **2001**, *17*, 481−488.
(13) Veisz, B.; Kiraly, Z. *Langmuir* **2003**, *19*, 4817−4824.
(14) Chen, M.; Falkner, J.; Guo, W.-H.; Zhang, J.-Y.; Sayes, C.; Colvin, V. L. *J. Colloid Interface Sci.* **2005**, *287*, 146−151.
(15) Narayanan, R.; El-Sayed, M. A. *J. Am. Chem. Soc.* **2003**, *125*, 8340−8347.
(16) Teranishi, T.; Miyake, M. *Chem. Mater.* **1998**, *10*, 594−600.
(17) Thomas, P. J.; Kulkarni, G. U.; Rao, C. N. R. *J. Phys. Chem. B* **2000**, *104*, 8138−8144.
(18) Son, S. U.; Jang, Y.; Yoon, K. Y.; Kang, E.; Hyeon, T. *Nano Lett.* **2004**, *4*, 1147−1151.
(19) Kim, S.-W.; Park, J.; Jang, Y.; Chung, Y.; Hwang, S.; Hyeon, T.; Kim, Y. W. *Nano Lett.* **2003**, *3*, 1289−1291.
(20) Hiramatsu, H.; Osterloh, F. E. *Chem. Mater.* **2004**, *16*, 2509−2511.
(21) Dey, S.; Jain, V. K. *Platinum Met. Rev.* **2004**, *48*, 16−29.
(22) Koizumi, N.; Miyazawa, A.; Furukawa, T.; Yamada, M. *Chem. Lett.* **2001**, *30*, 1282−1283.
(23) Capdevielle, P.; Lavigne, A.; Sparfel, D.; Baranne-Lafont, J.; Nguyen, Kim, C.; Maumy, M. *Tetrahedron Lett.* **1990**, *31*, 3305−3308.
(24) Murayama, H.; Ichikuni, N.; Negishi, Y.; Nagata, T.; Tsukuda, T. *Chem. Phys. Lett.* **2003**, *376*, 26−32.
(25) Teranishi, T.; Inoue, Y.; Nakaya, M.; Oumi, Y.; Sano, T. *J. Am. Chem. Soc.* **2004**, *126*, 9914−9915.
(26) Love, J. C.; Wolfe, D. B.; Haasch, R.; Chabinyc, M. L.; Paul, K. E.; Whitesides, G. M.; Nuzzo, R. G. *J. Am. Chem. Soc.* **2003**, *125*, 2597−2609.
(27) Samia, A. C. S.; Hyzer, K.; Schlueter, J. A.; Qin, C.-J.; Jiang, J. S.; Bader, S. D.; Lin, X.-M. *J. Am. Chem. Soc.* **2005**, *127*, 4126−4127.